

## Opposed shear senses inferred from neotectonic mesofracture systems in the North Anatolian fault zone

P. L. HANCOCK and A. A. BARKA

Department of Geology, University of Bristol, Queen's Building, University Walk, Bristol BS8 1TR, England

(Received 23 December 1980; accepted in revised form 9 May 1981)

**Abstract**—The 1200-km long North Anatolian fault zone is a right-lateral, intracontinental transform boundary which was initiated in the Late Neogene. Sediments of Pliocene to Holocene age in basins between Cerkes and Erbaa, within the convex-northwards arc of the fault zone, are deformed by syn-sedimentary and post-depositional mesoscopic faults and joints. The mesofractures, which strike obliquely to the fault zone, include reverse faults, normal faults, normal shear joints, conjugate vertical joints and strike-slip faults. Each type of structure occurs in two geometrical groups, one comprises four systems of fractures, the other is made up of five systems. The directions of secondary compression and/or extension inferred from the first group of mesofractures, which are restricted to sediments of Pliocene to Early Pleistocene age, are interpreted as being related to left-lateral shear along the North Anatolian fault zone. The directions of compression and/or extension inferred from the second group of mesofractures, which cut sediments of Pliocene to late Holocene age, were generated during right-lateral shear.

The presence of the second group of mesofractures is understandable because they are related to the shear sense which operates at the present-day, but those interpreted as being related to left-lateral shear are more puzzling: their development implies one or more reversals of the dominant sense of displacement. Several tentative models to explain such reversals are proposed, including regional and local influences, the latter related to mechanical constraints and/or the effects of other fault systems.

### PURPOSE AND SCOPE

FOCAL mechanism solutions (e.g. McKenzie 1972, Canitez 1973), the offset of man-made and physiographic features during earthquakes (e.g. Ketin 1948, Allen 1969, Ketin 1969, Ambraseys 1970, Şengör 1979) and the displacement of geological lines (e.g. Kopp *et al.* 1969, Tokay 1973, Seymen 1975, Şengör 1979) indicate that present-day displacements along the approximately 1200 km arc of the North Anatolian fault zone are right-lateral, and that since the Miocene there has been a substantial cumulative right-lateral displacement. According to McKenzie (1972) and Şengör (1979) the northwards motion of the Arabian plate is responsible for the westwards extrusion of the Anatolian plate; that is the region to the north of the eastern Mediterranean is experiencing indentation tectonics (Tapponnier & Molnar 1976). The northern boundary of the semi-rigid Anatolian plate is the right-lateral North Anatolian fault zone and the southern boundary is defined by the left-lateral East Anatolian fault, Cyprus, and the Pliny/Strabo and Hellenic trenches (Dewey & Şengör 1979, Şengör 1979, Şengör & Yilmaz 1981). (Fig. 1a).

This paper analyses several systems of mesoscopic-scale faults and joints which were investigated during a broader study of the seismology, physiography and structural geology of that part of the convex-northwards arc of the North Anatolian fault zone between Cerkes and Erbaa (Fig. 1b). Four of the six well-known 20th century active fault breaks associated with the westwards migrating epicentres of large-magnitude earthquakes occur within the approximately 450 km studied arc (Ketin 1948, Ambraseys 1970, Töksöz *et al.* 1979). Because we wished

to employ the mesofractures as kinematic indicators of displacements which have occurred since the Miocene, our survey was deliberately restricted to fractures cutting sediments of Pliocene or Quaternary age occupying basins within or adjacent to the fault zone. All of these Late Cenozoic sediments are of continental origin and were deposited in intermontane basins which were isolated from each other. Dating and correlation of the successions are less precise than in the Aegean region, where the sequences are marine.

On the basis of a study of the Neogene-early Pleistocene sediments in the Havza-Ladik and Tasova-Erbaa basins, Irrlitz (1972) proposed that they belong to the Pontus Formation, distinguishing between a Lower Pontus series of late Miocene-early Pliocene age and an Upper Pontus series of late Pliocene-early Pleistocene age. Although Irrlitz (1972) did not recognize a hiatus between the Lower and Upper Pontus series our survey has indicated the presence of an unconformity which is angular in many places close to the active trace of the North Anatolian fault. The sediments of the three western basins are thought to be broadly equivalent to those of the two eastern basins (Irrlitz 1971). The approximately 500 m Lower Pontus series comprises lacustrine sands, silts, clays and marls in the centres of basins, but it passes laterally into fluvial gravels and sands at their margins. The 300 m Upper Pontus series contains a greater proportion of coarse clastic material, so that, for example, gravels occur close to basin centres. Near Cerkes (Fig. 1b) the fluvial sediments of the Upper Pontus series pass laterally into colluvium (hill-wash) along basin margins.

Although there are no published details about the upper Pleistocene and Holocene successions our survey

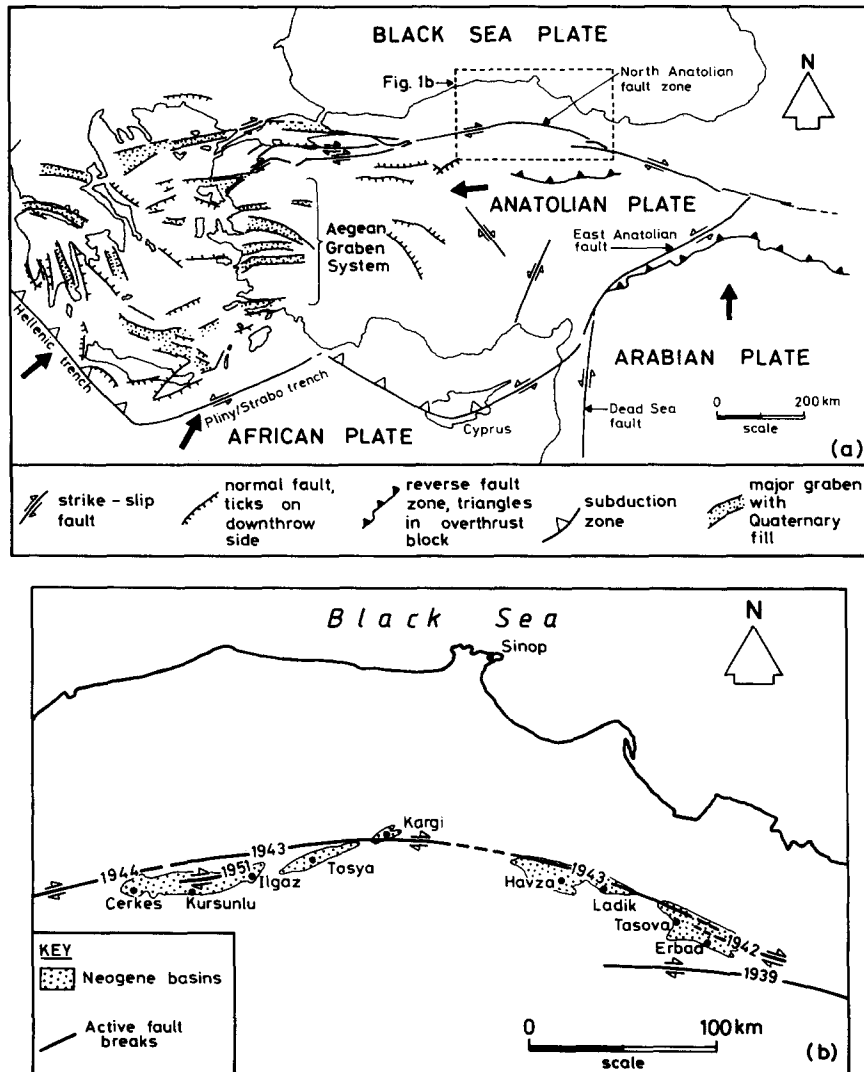


Fig. 1. (a) Tectonic setting of the North Anatolian fault zone (after Şengör 1979, fig. 1, Hancock & Barka 1980, fig. 1 a, and Le Pichon & Angelier in press, fig. 1). (b) Locations of the surveyed Neogene-Quaternary sedimentary basins and the traces of five fault breaks developed during 20th century large-magnitude earthquakes (dates given on the map). Generalised boundaries of the basins from the Zonguldak, Sinop and Samsun sheets of the 1 : 500,000 geological map of Turkey.

suggests that they are divisible into several levels of late Pleistocene-early Holocene terrace gravels, each of which is accompanied by alluvial fans and laterally equivalent colluvial deposits. Everywhere these sediments rest unconformably on the Pontus Formation. Late Holocene alluvial sediments complete the Cenozoic succession.

### DESCRIPTION OF THE MESOFRACTURE SYSTEMS

The orientations and morphological characteristics of 1941 mesofractures were recorded at 142 sampling sites (stations) scattered throughout the basins. Each station is a structurally homogeneous domain of less than 50 m<sup>2</sup> in which the inclination of sedimentary layering is uniform.

Five types of mesofractures are represented: (a) reverse faults; (b) normal faults; (c) steeply inclined joints; (d) vertical joints; and (e) strike-slip faults. All types belong

to two groups which may be distinguished from each other on the basis of their geometry and whether they occur only in the Pontus Formation, or whether they occur in both the Pontus Formation and the overlying upper Pleistocene-Holocene succession.

Group 1 mesofractures (Table 1) account for 27.3% of the total sampled and make up four systems: (a) conjugate reverse faults striking NW (1.0%, Fig. 2a); (b) conjugate normal faults striking NE (3.3%, Fig. 2b); (c) conjugate steeply inclined joints striking NE (3.3%, Fig. 2c) and (d) either conjugate vertical joints enclosing an acute angle about a NE trending bisector, or a single set of vertical joints striking NE (19.5%, Fig. 2d). Percentages given in parentheses refer to the proportion of fractures in a system as a percentage of the total sample of all mesofractures.

Group 2 mesofractures (Table 2) account for 47.2% of the total sampled; excluding strike-slip faults, they also define four systems directly comparable to those in

Table 1. Mean orientations of group 1 mesofracture sets and the mean orientations of  $\sigma_1$  and  $\sigma_3$  inferred from the sets

| Basin  | Reverse mesofaults |          |           | Normal mesofaults |          |          | Steeply inclined joints |               |          | Vertical joints |           |            | Fault zone trend |          |          |       |                  |            |
|--|--------------------|----------|-----------|-------------------|----------|----------|-------------------------|---------------|----------|-----------------|-----------|------------|------------------|----------|----------|-------|------------------|------------|
|  | set 1              | set 2    | $2\theta$ | $\sigma_1$        | set 1    | set 2    | $2\theta$               | $\sigma_3$    | set 1    | set 2           | $2\theta$ | $\sigma_3$ |                  | set 1    | set 2    | set 3 | $2\theta$        | $\sigma_3$ |
| -west<br>Cerkes-Ilgaz-centre                     | 156/68NE           | 154/62SW | 50°       | 065/03            | 019/79NW | 018/55SE | 46°                     | 320<br>289/11 | 081/64NW | 082/50SE        | 66°       | 351/06     | 055/89NW         | 095/85SW | 054/87SE | 0°    | 324/03<br>343/02 | 080<br>078 |
| -east<br>Tosya                                   | 132/25NE           | —        | —         | 042               | 016/70NW | 018/67SE | 44°                     | 287/01        | 029/72NW | 030/68SE        | 41°       | 299/01     | 014/89NW         | 051/88NW | —        | 37°   | 123/01           | 069        |
| Kargi  | —                  | —        | —         | —                 | 052/63NW | 047/84SE | 35°                     | 138/11        | 040/51NW | 044/74SE        | 56°       | 132/01     | 044/86SE         | 080/85SE | —        | 36°   | 331/04           | 079        |
| Havza-Ladik                                      | —                  | —        | —         | —                 | 066/53NW | 065/62SE | 74°                     | 335/01        | 075/68NW | 076/64SE        | 48°       | 345/03     | 034/81SE         | 100/87NE | —        | 65°   | 337/08           | 090        |
| Tasova-Erbaa                                     | —                  | —        | —         | —                 | 060/52NW | 050/48SE | 81°                     | 325/03        | —        | —               | —         | —          | 060/85NW         | 088/87SE | —        | 26°   | 336/04           | 110        |
| Total number of sampled fractures in each system | 20                 |          |           | 65                |          |          | 65                      |               |          | 380             |           |            |                  |          |          |       |                  |            |

Notes: Fracture orientations are given as three-digit azimuths of strike, two-digit angles of inclination and letters to indicate the direction of inclination. The mean orientation of each set in each basin (or part of the Cerkes-Ilgaz basin) was determined from the mean orientations of that set at numerous stations. Surfaces in sets 1 or 2 in each system are slicken planes and those in set 3 within the system of vertical joints are extension fractures.  $\sigma_1$  (maximum principal stress) and  $\sigma_3$  (minimum principal stress) are given as three-dimensional orientations. From single sets of shear fractures the horizontal projection of  $\sigma_1$  or  $\sigma_3$  has been taken to be approximately normal to the strike of the set.  $2\theta$  is the mean conjugate shear angle.

Table 2. Mean orientations of group 2 mesofracture sets (excluding strike-slip faults) and the mean orientations of  $\sigma_1$  and  $\sigma_3$  inferred from the sets

| Basin  | Reverse mesofaults |          |           | Normal mesofaults |          |          | Steeply inclined joints |            |          | Vertical joints |           |            | Fault zone trend |       |          |       |                  |            |
|--|--------------------|----------|-----------|-------------------|----------|----------|-------------------------|------------|----------|-----------------|-----------|------------|------------------|-------|----------|-------|------------------|------------|
|  | set 1              | set 2    | $2\theta$ | $\sigma_1$        | set 1    | set 2    | $2\theta$               | $\sigma_3$ | set 1    | set 2           | $2\theta$ | $\sigma_3$ |                  | set 1 | set 2    | set 3 | $2\theta$        | $\sigma_3$ |
| -west<br>Cerkes-Ilgaz-centre                     | —                  | 056/53SE | —         | 146               | 143/72NE | 166/79SW | 38°                     | 245/02     | 120/51NE | 115/59SW        | 72°       | 207/03     | —                | —     | 154/85NE | 0°    | 064/05<br>061/08 | 080<br>078 |
| -east<br>Tosya                                   | 011/29NW           | 010/40SE | 80°       | 100/01            | 166/53NE | 165/55SW | 72°                     | 255/02     | 151/62NE | 163/48SW        | 71°       | 067/06     | —                | —     | 151/82SW | 0°    | 250/01           | 069        |
| Kargi  | 023/78NW           | —        | —         | 113               | 113/83NE | —        | —                       | 023        | 142/73NE | 139/70SW        | 37°       | 050/01     | —                | —     | 147/87NE | 0°    | 057/03           | 079        |
| Havza-Ladik                                      | 056/18NW           | 026/24SE | 40°       | 129/03            | 154/67NE | 147/71SW | 46°                     | 241/02     | 140/67NE | 146/54SW        | 60°       | 054/06     | —                | —     | 151/87NE | 0°    | 061/03           | 090        |
| Tasova-Erbaa                                     | 039/53NW           | 038/40SE | 92°       | 309/05            | 000/59E  | 006/79W  | 54°                     | 274/09     | 159/74NE | 154/71SW        | 36°       | 276/08     | —                | —     | 142/87SW | 0°    | 052/03           | 110        |
| Total number of sampled fractures in each system | 33                 |          |           | 146               |          |          | 305                     |            |          | 405             |           |            |                  |       |          |       |                  |            |

Note: For meanings of symbols and conventions see Table 1.

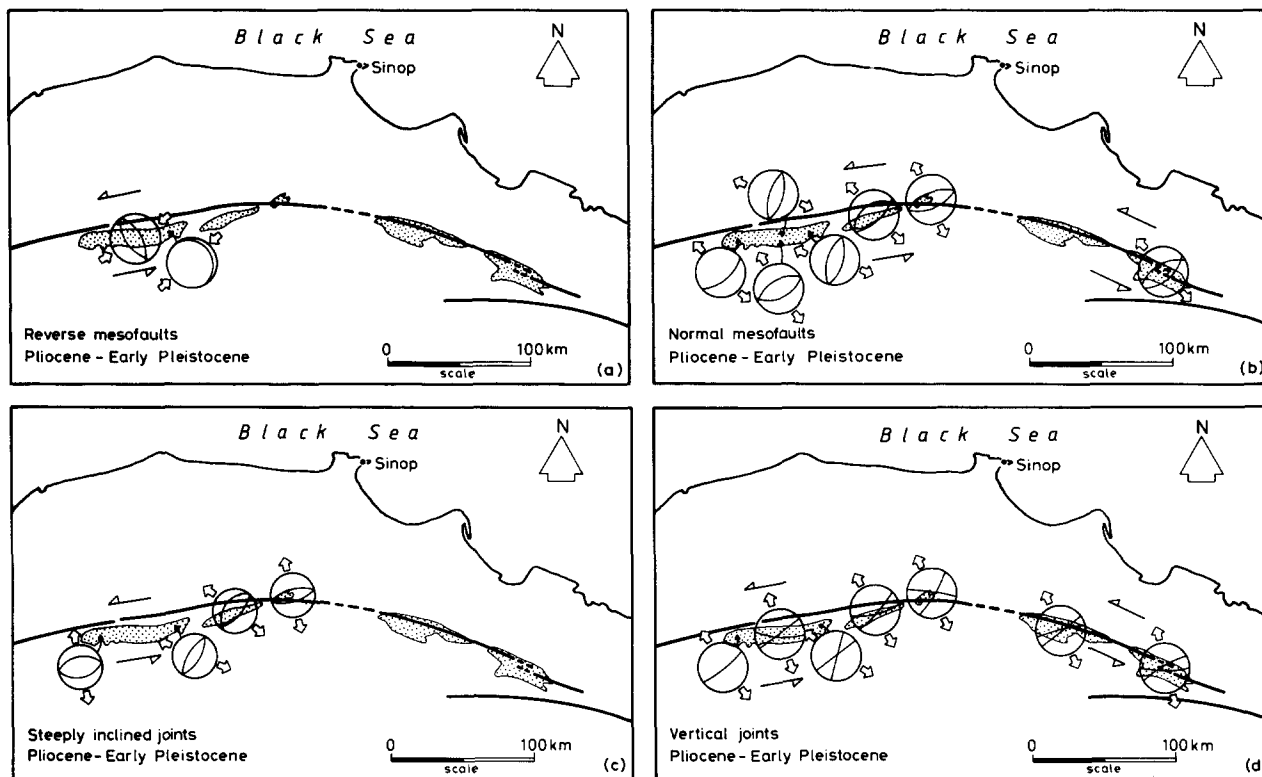


Fig. 2. Mean cyclographic traces of group 1 mesofractures of Pliocene-early Pleistocene age and from which a left-lateral sense of displacement on the North Anatolian fault zone may be inferred. Basins and fault traces as in Fig. 1(b). Stereograms are lower-hemisphere Lambert plots of fracture sets after rotation by the same amount and in the same sense as that required to restore beds to the horizontal. Arrow pairs immediately external to each plot show the horizontal projections of the three-dimensional orientations of compression or extension axes (see Table 1). (a) Reverse mesofaults. (b) Normal mesofaults. (c) Steeply inclined joints. (d) Vertical joints. Modified after Hancock & Barka (1980, fig. 3).

group 1. The systems are: (a) conjugate reverse faults striking NE (1.7%, Fig. 3a); (b) conjugate normal faults striking NW (7.5%, Fig. 3b); (c) conjugate steeply inclined joints striking NW (15.7%, Fig. 3c) and (d) either conjugate vertical joints enclosing an acute angle symmetrically about a NW trending bisector, or a single set of vertical joints striking NW (20.8%, Fig. 3d).

The mean orientations (Tables 1 and 2) of the sets in the eight systems in each basin or part of a basin are plotted as cyclographic traces in Figs. 2 and 3, and, in both the tables and the figures, are shown after stereographic rotation by the same amount and in the same sense as that required to restore beds to the horizontal. The rotations of the observed orientations do not imply that we believe the structures were initiated in horizontal sediments which were subsequently tilted. They were carried out so that geometrical comparisons of fractures symmetrically related to layering could be made between sediments tilted at different angles. Because at the majority of stations the sediments dip at less than  $20^\circ$  there is little distinction between the observed and rotated orientations.

The reason why two systems of normal faults or steeply inclined joints are shown for the Cerkes-Ilgaz and Havza-Ladik basins (Figs. 2b and 3b & c) is that within those basins it is possible to distinguish between the attitudes of two subsystems of faults or joints in each system.

All of the sampled structures are of mesoscopic scale, that is, they are either joints or small faults of less than  $30\text{ m}^2$  and/or less than 3 m displacement (Fig. 4). Only 7.6% of the faults are striated, this low percentage of striated surfaces may be a consequence of the clastic sediments which they cut being unconsolidated or weakly consolidated. At some stations in the Pontus Formation there are syn-sedimentary faults (e.g. Figs. 4d & e) while at others (e.g. Figs. 4b & c) the fractures appear to be post-depositional in that they cut the exposed part of the Pontus succession. However, some of these fractures may be syn-sedimentary although the relevant evidence has been removed and replaced by an erosion surface between the Pontus Formation and overlying colluvium or soil. At most localities (e.g. Figs. 4b & c) fault scarps were denuded before the accumulation of colluvium or soil, and hence it is likely that faulting had ceased well before the late Quaternary. At the locality illustrated in Fig. 4(f) a fault-line scarp in the Upper Pontus series is buried by colluvium; faulting at that locality may have continued until the late Quaternary because both sides of the scarp are underlain by gravels of the same resistance to erosion.

Figure 5 shows the restored mean attitudes of group 2 high-angle mesofaults (1.4% of the total sample of 1941 surfaces) which strike at small angles to the main trace of the North Anatolian fault and which show either strike-slip offsets or, more rarely (8.4% of the category),

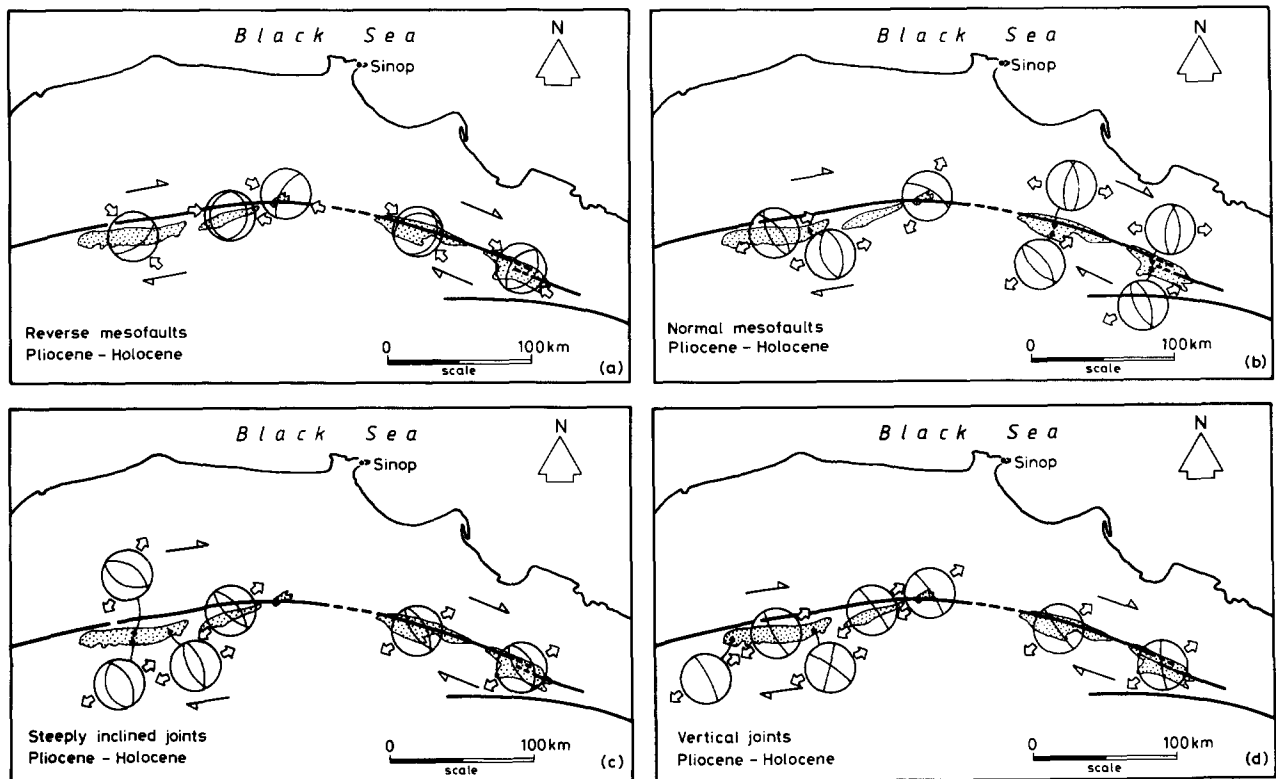


Fig. 3. Mean cyclographic traces of group 2 mesofractures of Pliocene-Holocene age and from which a right-lateral sense of displacement on the North Anatolian fault zone may be inferred. All conventions as in Fig. 2. (a) Reverse mesofaults. (b) Normal mesofaults. (c) Steeply inclined joints. (d) Vertical joints.

nearly horizontal slickenside striations. Seventy-five per cent of group 2 strike-slip mesofaults are right-lateral shears as inferred from displacements or congruous asymmetric steps on their surfaces.

Mesofractures in group 1 (Fig. 2) are restricted to the Pontus Formation in which they are more abundant in the lower series. Their restricted stratigraphical distribution, coupled with the observation that both syn-sedimentary and post-sedimentary faults are represented, allows the inference that group 1 mesofractures were developed episodically throughout the Pliocene and early Pleistocene, with most activity occurring during the earlier part of that time interval. Because of the difficulty of correlating different horizons within the Pontus Formation it is not possible to recognize widespread individual episodes of compression or extension.

Syn-sedimentary and post-depositional mesofractures belonging to group 2 (including the strike-slip faults) occur in both the Pontus Formation and the overlying Late Pleistocene and Holocene successions, although above the Pontus Formation they are restricted to relatively narrow belts adjacent to active fault breaks (not necessarily the main active trace of the North Anatolian fault). Some of the youngest group 2 normal mesofaults are expressed by fault scarps visible in the field. We conclude that group 2 mesofractures were initiated episodically throughout the basins, from the Pliocene to the end of the early Pleistocene, and that their initiation continued in restricted belts until the late Holocene.

At the few stations where mesofractures in both groups occur in association, those in group 1 are generally cut by those in group 2, and hence the oldest fractures in any basin are likely to belong to group 1. However, it should be emphasised that because both groups contain syn-sedimentary faults it is likely that all mesofractures were generated throughout much of Pliocene-early Pleistocene time, and those in group 2 continued to be initiated from the late Pleistocene onwards.

## STRUCTURAL INTERPRETATION OF THE MESOFRACTURE SYSTEMS

### Principles

The value of analysing mesofractures in order to determine regional palaeostress/strain trajectories is well known (e.g. Hancock & Kadhi 1978, Hancock & Atiya 1979, Letouzey & Trémoilières 1980). Although some of the fractures discussed in this paper are syn-sedimentary and others are post-depositional they are all regarded as being of tectonic origin because they are uniformly orientated with reference to the trend of the North Anatolian fault zone. On the basis of geometry and/or whether they show displacements it is possible to allocate the majority of mesofractures to either a system of conjugate shears or a set of extension fractures. From conjugate sets of reverse mesofaults the orientation of the

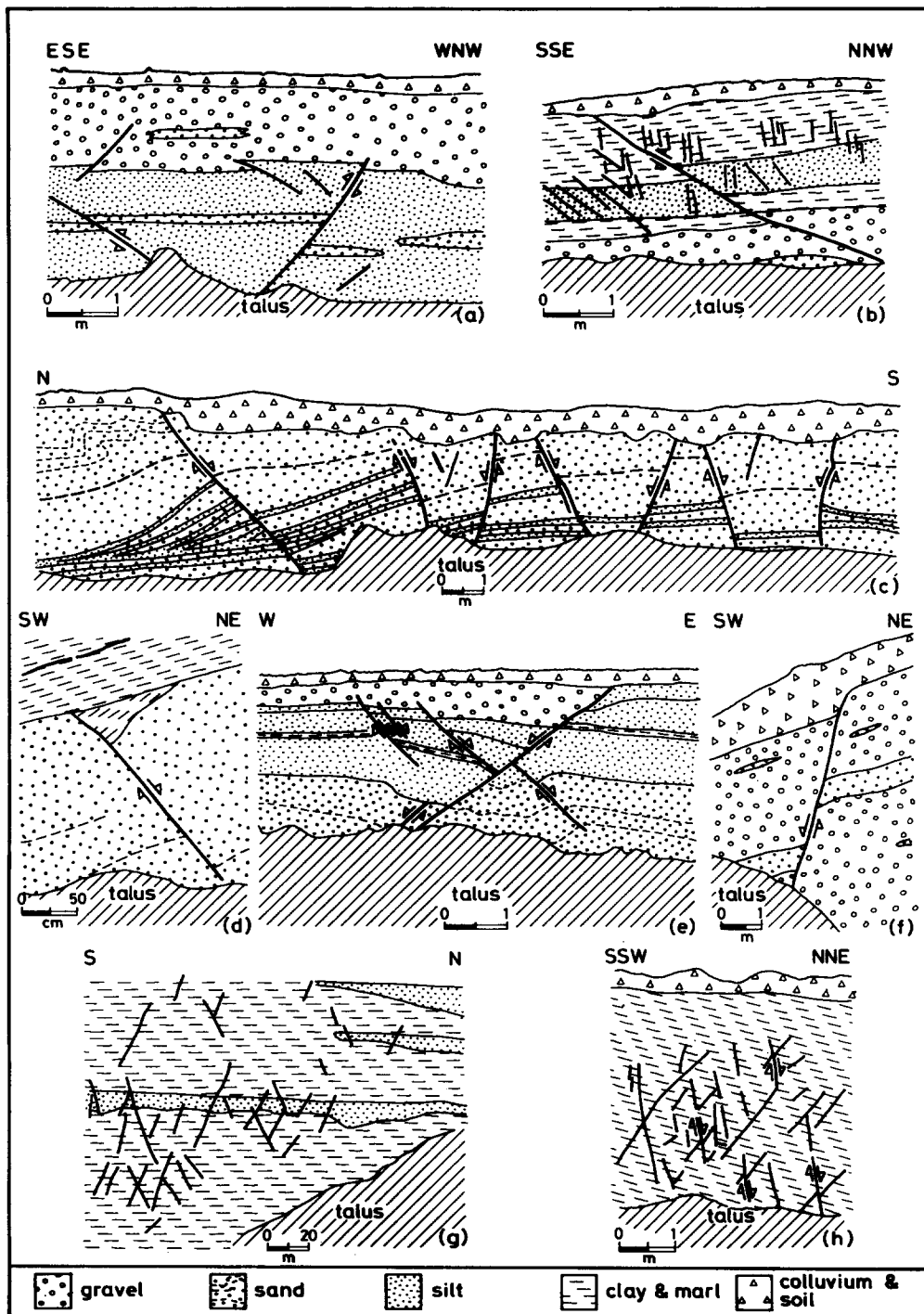


Fig. 4. Sketches from photographs of group 1 and 2 mesofractures within the North Anatolian fault zone. (a) Conjugate group 1 reverse mesofaults in the Lower Pontus series about 5 km west of Kursunlu. (b) A group 2 reverse mesofault and associated joints in the Lower Pontus series about 7.5 km northeast of Havza. Joints parallel to reverse mesofaults are rare and restricted to zones within a few metres of reverse faults. (c) Conjugate group 1 normal mesofaults in the Lower Pontus series at Kursunlu. Note the syn-sedimentary folds at the northern end of the section. (d) A syn-sedimentary group 2 normal mesofault in the Lower Pontus series about 12 km northwest of Havza. (e) Conjugate group 2 normal mesofaults in the Lower Pontus series about 12.5 km east of Kursunlu. Note the X pattern formed by two of the conjugate faults which cross each other, and that faults in the east-dipping set are syn-sedimentary. (f) A group 2 normal mesofault in the Upper Pontus series about 8 km northeast of Havza. A resequent fault-line scarp is buried by late Quaternary colluvium. (g) Conjugate group 1 steeply inclined (normal) shear joints in the Lower Pontus series about 3 km southeast of Tosya. (h) Conjugate group 2 steeply inclined (normal) shear joints and microfaults in the Upper Pontus series at Erbaa. Figs. 3(a), (c) and (g) from Hancock & Barka (1980, fig. 2).

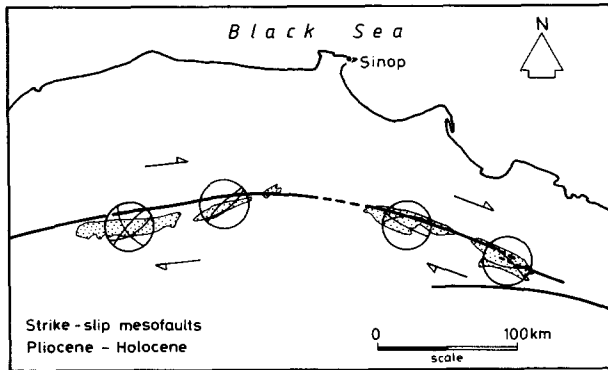


Fig. 5. Mean cyclographic traces of group 2 strike-slip faults of meso-scale in sediments of Pliocene to Holocene age. Stereograms are lower-hemisphere Lambert plots of sets after rotation with bedding restored to the horizontal. Basins and fault traces as in Fig. 1(b).

acute bisector gives the three-dimensional attitude of the maximum principal stress ( $\sigma_1$ ). From a single set of reverse mesofaults the approximate direction of the horizontal projection of  $\sigma_1$  was taken to be normal to the mean strike of the set. The orientation of the minimum principal stress ( $\sigma_3$ ) was taken to be identical to that of the obtuse bisector between conjugate sets of: (a) mesofaults; (b) steeply inclined joints or (c) vertical joints. From a single set of normal mesofaults the approximate direction of the horizontal projection of  $\sigma_3$  was taken to be at right angles to the mean strike of the set. Single sets of vertical extension joints are regarded as having been initiated normal to  $\sigma_3$ . The above geometrical techniques for determining principal stress directions possess some inherent uncertainties. First, they are theoretically valid only when the fractures cut mechanically isotropic rocks (Anderson 1951). However, the experience of many field workers (e.g. Hancock & Kadhi 1978, Letouzey & Trémoilières 1980) is that the presence of an older mesofracture set does little to influence the development of a younger mesofracture set. Secondly, as has been argued by Mercier *et al.* (1973) and Angelier (1979), it is preferable to determine principal strain or stress axes from faults which are striated. Because only 7.6% of the faults analysed in this paper are striated and because 59.3% of fractures in groups 1 and 2 are joints (which by definition cannot be striated) we were unable to use their more exact techniques. However, Anderson's (1951) technique for inferring principal stress directions is sufficiently precise and yields results which are consistent within and between basins. We have determined principal stress directions rather than principal strain directions because for the latter to be regionally significant, it is necessary to know both the attitudes of the planar structures and the net displacement on each set. If one set is better developed than another, the  $X$  and  $Z$  axes of the strain ellipsoid will be rotated away from the obtuse and acute bisectors between the planes.

#### Mechanical interpretation of the types of mesostructures in groups 1 and 2

The average acute shear angle ( $2\theta$ , Tables 1 and 2)

between conjugate sets of reverse faults, normal faults and steeply inclined joints generally exceeds  $45^\circ$ , and thus the surfaces are interpreted as shear planes rather than extension fractures. Those enclosing an average  $2\theta$  angle between  $45$  and  $59^\circ$  are probably hybrid fractures belonging to the shear-extension fracture transition (see e.g. Hancock & Kadhi 1978). Vertical joints comprise either single sets of extension fractures (for which  $2\theta$  may be thought of as being  $0^\circ$ , see Tables 1 and 2) or conjugate fracture sets in which  $2\theta$  is generally less than  $45^\circ$  in group 1 (sets 1 and 2, Table 1) but within a few degrees of  $60^\circ$  in group 2 (sets 1 and 2, Table 2). Thus conjugate group 1 vertical joints are interpreted as hybrid fractures whereas conjugate group 2 vertical joints are regarded as shears. Steeply inclined joints which are subparallel to nearby normal mesofaults are interpreted as normal shear joints.

#### Group 1 mesofractures

Figure 2 shows the horizontal projections of the directions of compression ( $\sigma_1$ ) or extension ( $\sigma_3$ ) inferred from the four systems of group 1 mesofractures. The directions of  $\sigma_1$  or  $\sigma_3$  are oblique to the trend of the fault zone and their arrangement is consistent with predicted directions of secondary compression or extension which would be generated within a nearly vertical fault zone along which there was left-lateral shear. Figure 6(a) shows schematically a mechanical interpretation of group 1 mesofractures with reference to an E-W trending fault zone along which there has been left-lateral shear.

As Fig. 2 reveals, group 1 mesofractures are not uniformly distributed along the fault zone, 79% of them occurring in the three western basins. The two subsystems of normal mesofaults in the central part of the Cerkes-Ilgaz basin (Fig. 2b and Table 1) were probably formed during separate episodes of left-lateral shear, each of which resulted in a slightly different direction of secondary extension.

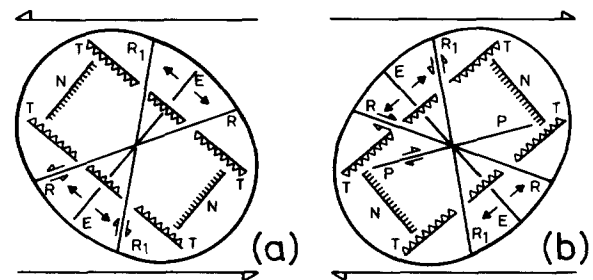


Fig. 6. Mechanistic interpretation of neotectonic mesofractures associated with the North Anatolian fault zone between Cerkes and Erbaa. For simplicity the fault zone is shown trending E-W. (a) Group 1 mesofractures related to left-lateral shear. (b) Group 2 mesofractures related to right-lateral shear. Systems are indicated by initials; T, conjugate reverse mesofaults; N, conjugate normal mesofaults and steeply inclined joints; E, vertical extension joints; R, vertical Riedel shear joints and strike-slip faults;  $R_1$ , vertical  $R_1$  Riedel shear joints and strike-slip faults; P, vertical strike-slip faults of P shear orientation.

### Group 2 mesofractures

The horizontal projections of  $\sigma_1$  or  $\sigma_3$  axes inferred from group 2 reverse and normal mesofaults, steeply inclined joints and vertical joints are shown in Fig. 3. These directions are arranged in the opposite manner to those of  $\sigma_1$  and  $\sigma_3$  inferred from group 1 mesofractures, and hence their arrangement is in accord with their being secondary directions of compression or extension related to right-lateral shear along the North Anatolian fault zone (Fig. 6b). The directions of  $\sigma_3$  inferred from group 2 mesofractures are comparable with the directions of extension axes determined from focal mechanism solutions (e.g. McKenzie 1972, Canitez 1973) of earthquakes which have occurred on the North Anatolian fault zone during its present phase of seismic activity.

Group 2 strike-slip mesofaults with trends that face against the dominant right-lateral sense of shear along the fault zone are interpreted as Riedel shears while those striking with the shear sense are interpreted as *P* shears (Fig. 6b) (cf. Tchalenko & Ambraseys 1970). Both *P* and *R* shears are present in the two eastern basins but only *P* shears are represented in the two westernmost basins. The NNW-SSE trending strike-slip mesofault in the central part of the Cerkes-Ilgaz basin may be  $R_1$  shears (Fig. 6b). In common with other parts of the North Anatolian fault zone (e.g. the Mudurnu valley, Ambraseys 1970) there are remarkably few meso-scale strike-slip faults precisely parallel to the main trace of the earthquake fault zone.

Mesofractures belonging to group 2 are more widely distributed than those of group 1 (Figs. 3 and 5), and this observation, coupled with their occurrence in sediments of early Pliocene to late Holocene age, allows the conclusion that right-lateral displacement has been the dominant mode of shear along the entire length of the North Anatolian fault zone since its inception. The paired subsystems of normal mesofaults in the Havza-Ladik and Tasova-Erbaa basins (Fig. 3b) and the paired subsystems of steeply inclined joints in the central part of the Cerkes-Ilgaz basin (Fig. 3c) probably reflect slightly different directions of secondary extension during separate episodes of right-lateral shear.

## TECTONIC IMPLICATIONS

Although we have not conducted a detailed mesofracture study in the Neogene/Quaternary sediments of basins immediately external to the North Anatolian fault zone our reconnaissance survey indicates that their arrangement is unlike that in the basins along the fault zone. Thus it is likely that the mesofractures analysed in this paper are restricted to the North Anatolian fault zone and that their genesis is related to the evolution of the zone.

The widespread areal and temporal distribution of group 2 mesofractures, interpreted as being related to directions of secondary compression or extension generated during episodic right-lateral shear since the be-

ginning of the Pliocene, is understandable because that inferred shear sense accords with the present-day sense of displacement along the North Anatolian fault zone. However, the presence of group 1 mesofractures is more puzzling and their interpretation may be of more than local interest; comparable anomalously trending structures having been reported by Bishop (1968, fig. 5) from between two strands of the Alpine fault in New Zealand. The observation that, apart from their orientations, mesofractures in group 1 resemble those in group 2 suggests that they were generated in a similar manner: that is they are structures related to directions of secondary compression or extension within a broad strike-slip fault zone. The orientations of group 1 mesofractures are those which would be anticipated if the sense of shear along the major fault zone had been left-lateral, either regionally or locally. Hancock & Barka (1980), in a preliminary note on mesofractures in group 1, proposed two possible explanations for such a reversal (or reversals) of the dominant sense of displacement along the North Anatolian fault zone. Here we expand on this theme, first considering regional explanations and secondly local explanations for the occurrence of the 'anomalous' fractures.

### Regional reversals

It is possible that the inferred changes in the sense of shear along the North Anatolian fault zone are related to alternating episodes of compression or extension which may have affected other parts of the Anatolian-Aegean plate. For example, the southern and southwestern magmatic domains of the Aegean region have experienced such alternating phases according to Mercier (1977) and Le Pichon & Angelier (in press). However, despite the attractions of a hypothesis attempting to link tectonic behaviour in the Aegean region with that along the North Anatolian fault, the conclusions of the French neotectonic schools are at variance with those of Dewey & Şengör (1979) and Şengör & Yılmaz (1981) who, in their analyses of the Aegean and Turkish regions, do not find evidence in favour of such reversals. A further objection to linking behaviour in the Aegean with that along the North Anatolian fault is that it is not possible to correlate the dated Aegean reversals with events along the North Anatolian fault zone.

### Local reversals

Because the majority of group 1 fractures occur in the three western basins it is likely that the left-lateral shearing to which they are related was concentrated along the western segment of the North Anatolian fault zone. In this connection it is noteworthy that the western segment of the fault zone is closer to the Aegean region, that part of the Anatolian plate which has experienced approximately N-S elongation (McKenzie 1972, Dewey & Şengör 1979), and is located on the restraining side of the convex-northwards arc. These factors may have given rise to



differences in behaviour between the western and eastern parts of the fault zone.

Şengör (personal communication 1980) has proposed that the evidence for left-lateral shear may be a consequence of the coincidence in plan between the western segment of the North Anatolian fault zone and one, or more, left-lateral fault zones which are known to characterize the more internal parts of the Anatolian plate (see Şengör 1979, fig. 6).

Three purely mechanistic explanations also require mention. First, as suggested by Price (1968), it is possible for normal dip-slip faults striking against a sense of transcurrent shear to develop as second-order structures depending upon factors such as the value of the vertical principal stress, the pore water pressure and the inertial stresses. Secondly, some group 1 mesofractures, especially joints, may be stress release structures formed after group 2 fractures which were generated during right-lateral shear. Although these two interpretations of group 1 fractures are appealing because they do not involve large-scale tectonic implications, they are difficult to reconcile with the stratigraphic evidence for group 1 mesofractures being restricted to the Pontus Formation; many mechanical influences are as likely to have operated since the deposition of the Pontus Formation as during it. Further, they cannot account for all the types or sets of group 1 mesofractures. The third mechanistic explanation possesses the merits of accounting for some of the objections raised to the first two. During episodes of right-lateral shear along the North Anatolian fault zone localised left-lateral shear may have been induced by pre-existing structures or buried, rigid blocks, which because of their attitudes, acted as buttresses capable of deflecting the local motion. A similar explanation, but involving larger-scale structures, has been put forward by Ambraseys (1975) to account for comparable tectonic complexities in the Zagros Ranges. With each episode of right-lateral shear on the North Anatolian fault zone it is likely that the asperities introduced by the buttresses would become less pronounced and increasingly localised, until in the late Pleistocene–Holocene they were insignificant and incapable of generating group 1 mesofractures; structures not observed in sediments younger than the early Pleistocene.

## CONCLUSIONS

The widespread development of group 2 mesostructures within the North Anatolian fault zone indicates that throughout much of Pliocene–Holocene time the sense of displacement was right-lateral. The presence of group 1 mesofractures, restricted to the Pontus Formation, shows that regionally or locally there were several subordinate episodes of left-lateral shear during the Pliocene and early Pleistocene. The imperfect state of knowledge about the structural evolution of Anatolia make it impossible for us to distinguish between the merits of regional or local explanations for there having been some left-lateral shear along all or part of the fault zone.

*Acknowledgements*—We are most grateful to N. N. Ambraseys, J. Angelier and A. M. C. Şengör for their many penetrating comments on a draft of this paper; nevertheless we take full responsibility for our interpretation. The M.T.A. Institute of Ankara financed fieldwork for both of us and provided a postgraduate award for one of us (A.A.B.). Jean Bees drafted the figures.

## REFERENCES

- Allen, C. R. 1969. Active faulting in northern Turkey. *Contr. No. 1577. Div. Geol. Sci., Calif. Inst. Tech.* 1–32.
- Ambraseys, N. N. 1970. Some characteristic features of the Anatolian fault zone. *Tectonophysics* **9**, 143–165.
- Ambraseys, N. N. 1975. Studies in historical seismicity and tectonics. In: *Geodynamics Today*. The Royal Society, London, 7–16.
- Anderson, E. M. 1951. *The Dynamics of Faulting (2nd Ed.)* Oliver & Boyd, Edinburgh.
- Angelier, J. 1979. Determination of the mean principal directions of stresses for a given fault population. *Tectonophysics* **56**, T17–T26.
- Bishop, D. G. 1968. The geometric relationships of structural features associated with major strike-slip faults in New Zealand. *N.Z. J. Geol. Geophys.* **11**, 405–417.
- Canitez, N. 1973. Yer kabuk hareketlerine ilişkin calismalar ve Kuzey Anadolu fayi problemi. In: *Symposium on the North Anatolian Fault and Earthquake Belt*. M.T.A. Enstitusu, Ankara.
- Dewey, J. F. & Şengör, A. M. C. 1979. Aegean and surrounding regions: complex multiplate and continuum tectonics in a convergent zone. *Bull. geol. Soc. Am.* **90**, 84–92.
- Hancock, P. L. & Atiya, M. S. 1979. Tectonic significance of mesofracture systems associated with the Lebanese segment of the Dead Sea transform fault. *J. Struct. Geol.* **1**, 143–153.
- Hancock, P. L. & Barka, A. A. 1980. Plio-Pleistocene reversal of displacement on the North Anatolian fault zone. *Nature, Lond.* **286**, 591–594.
- Hancock, P. L. & Kadhi, A. 1978. Analysis of mesoscopic fractures in the Dhurma–Nisah segment of the central Arabian graben system. *J. geol. Soc. Lond.* **135**, 339–347.
- Irritz, W. 1971. Neogene and Older Pleistocene of the intramontane basins in the Pontic region of Anatolia. *Newsl. Stratigr.* **1**, 33–35.
- Irritz, W. 1972. Lithostratigraphie und tektonische entwicklung des Neogens in Nordostanatolien. *Beih. geol. Jb.* **120**, 1–111.
- Ketin, I. 1948. Über die tectonisch-mechanischen Folgerungen aus den grossen Anatolischen Erdbeben des letzten Dezenniums. *Geol. Rdsch.* **36**, 77–83.
- Ketin, I. 1969. Über die Nordanatolische horizontalverschiebung. *Bull. Miner. Res. Explor. Inst., Ankara* **72**, 1–28.
- Kopp, K.-O., Pavoni, M. & Schindler, C. 1969. Geologie Thrakiens IV: das Ergene-Becken. *Beih. geol. Jb.* **76**, 1–136.
- Le Pichon, X. & Angelier, J. in press. The Aegean Sea. *Phil. Trans. R. Soc. Lond.*
- Letouzey, J. & Trémoières, P. 1980. Palaeo-stress fields around the Mediterranean since the Mesozoic derived from microtectonics: comparison with plate tectonic data. *Bull. Bur. Rech. géol. & Minières (Fr.)* **115**, 259–273.
- McKenzie, D. 1972. Active tectonics of the Mediterranean region. *Geophys. J. R. astr. Soc.* **30**, 109–185.
- Mercier, J. 1977. L'arc Egéen, une bordure déformée de la plaque Eurasiatique. Réflexions sur un exemple d'étude neotectonique. *Bull. Soc. géol. Fr., 7 Ser.* **19**, 663–672.
- Mercier, J., Vergely, P. & Delibassis, N. 1973. Comparisons between deformation deduced from the analysis of recent faults and from focal mechanisms of earthquakes (an example: the Paphos region, Cyprus). *Tectonophysics* **19**, 315–332.
- Price, N. J. 1968. A dynamic mechanism for the development of second order faults. *Geol. Surv. Pap. Can.* **68–52**, 49–78.
- Şengör, A. M. C. 1979. The North Anatolian fault: its age, offset and tectonic significance. *J. geol. Soc. Lond.* **136**, 269–282.
- Şengör, A. M. C. & Yilmaz, Y. 1981. Tethyan evolution of Turkey: a plate tectonic approach. *Tectonophysics* **75**, 181–241.
- Seymen, I. 1975. Kelkit Vadisi Kesiminde Kuzey Anadolu fay zonunun tektonik ozelligi. Doctoral thesis, Technical University of Istanbul.
- Tapponnier, P. & Molnar, P. 1976. Slip-line field theory and largescale continental tectonics. *Nature, Lond.* **264**, 319–324.
- Tchalenko, J. S. & Ambraseys, N. N. 1970. Structural analysis of the Dasht-e Bayaz (Iran) earthquake fractures. *Bull. geol. Soc. Am.* **81**, 41–60.

Tokay, M. 1973. Kuzey Anadolu fay zonunun Gerede ile Ilgaz arasındaki kisminda jeolojik gözlemler. In: *Symposium on the North Anatolian Fault and Earthquake Belt*. M. T. A. Enstitüsü, Ankara.

Töksöz, M. N., Şakal, A. F. & Michael, A. J. 1979. Space-time migration of earthquakes along the North Anatolian fault zone and seismic gaps. *Pageophys.* 117, 1258–1270.